Progress In Electromagnetics Research, PIER 25, 39–51, 2000

EXTINCTION BEHAVIOR OF DRY SNOW AT MICROWAVE RANGE UP TO 90 GHZ BY USING STRONG FLUCTUATION THEORY

H. Wang, J. Pulliainen, and M. Hallikainen

Laboratory of Space Technology
Helsinki University of Technology
P.O. Box 3000
FIN-02015, Finland

1. INTRODUCTION

In the modeling of microwave remote sensing observation, the radiative transfer theory has been applied to studies of scattering and emission from snow [1–3]. A key parameter in the radiative transfer equation is the extinction coefficient, also known as the power attenuation coefficient. The total loss of a medium is expressed by the extinction coefficient, which includes both the absorption loss and the scattering loss. At low frequencies absorption is the primary loss process, whereas at high frequencies scattering dominates over absorption. In order to investigate the properties of snow at high frequencies, the effect of scattering between ice particles must be taken into account. We employ here the strong fluctuation theory to solve such a problem.

The strong fluctuation theory has been extensively studied by several groups [4–8]. In the strong fluctuation theory, an inhomogeneous layer can be modeled as a continuous medium. Random medium is described by a correlation function, with the variance characterizing the strength of the permittivity fluctuations of the medium and correlation lengths corresponding to the scales of the fluctuations. Dry snow is a mixture of ice particles and air. Thus, a snowpack can be considered as a random medium. We can use strong fluctuation theory to calculate the extinction coefficient, phase matrix and effective permittivity of snow.

The aim of this paper is to examine the extinction behavior of dry snow in the 18 to 90 GHz range by using the strong fluctuation theory. Two extinction coefficient models are used in this study. In the model of Hallikainen et al. [9], the effective permittivity of dry snow is calculated by using strong fluctuation theory. The other modeling approach discussed in this paper employs phase matrices in the strong fluctuation theory to calculate the extinction coefficient. Phase matrices and scattering coefficients for spherical symmetric correlation function are derived in this paper. These formulas can also be used in radiative transfer equations to calculate the emissivity of dry snow.

The results of calculated extinction coefficients by using the two models are compared with the experimental data in the 18 to 90 GHz range. The experimental data of snow extinction coefficient are adopted from [9].

2. EXTINCTION COEFFICIENTS USING PHASE MATRIX IN STRONG FLUCTUATION THEORY

Consider scatterers with permittivity ε_s embedded in a background medium with permittivity ε_b. In the case of dry snow, the scatterers are ice particles and the background is air. The fraction volume occupied by the scatterers is f_ν and the fraction volume occupied by the background medium is $1 - f_\nu$. In the strong fluctuation theory, for a spherical symmetric correlation function, the quasi-static permittivity ε_g is determined by the following equation [4]:

$$f_\nu \left(\frac{\varepsilon_s - \varepsilon_g}{\varepsilon_s + 2\varepsilon_g} \right) + (1 - f_\nu) \cdot \left(\frac{\varepsilon_b - \varepsilon_g}{\varepsilon_b + 2\varepsilon_g} \right) = 0 \tag{1}$$

The variance of the fluctuation δ is [4]:

$$\delta = 9\frac{\varepsilon_g^2}{\varepsilon_0^2}\left[f_\nu\left(\frac{\varepsilon_s-\varepsilon_g}{\varepsilon_s+2\varepsilon_g}\right)^2+(1-f_\nu)\cdot\left(\frac{\varepsilon_b-\varepsilon_g}{\varepsilon_b+2\varepsilon_g}\right)^2\right] \tag{2}$$

Now we use the fluctuation theory to calculate the phase matrix and extinction coefficient. The extinction coefficient $\kappa_{e\nu}$ is defined as [9]:

$$\kappa_{e\nu} = \kappa_a + \kappa_{s\nu} \tag{3}$$

where κ_a is the absorption coefficient and $\kappa_{s\nu}$ is the scattering coefficient; subscribe ν denotes the ν polarization. The absorption coefficient κ_a is defined as [9]:

$$\kappa_a = 2k_0 \mathrm{Im}\left[\left(\frac{\varepsilon_g}{\varepsilon_0}\right)^{\frac{1}{2}}\right] \tag{4}$$

where k_0 is the wave number of free space; ε_g is the quasi-static value of the dielectric constant of dry snow.

The scattering coefficients $\kappa_{s\nu}$ and κ_{sh} are deduced from the phase matrix components [5]

$$\kappa_{s\nu}(\theta) = \int_0^\pi d\theta' \sin\theta' \left[P_{11}(\theta,\theta') + P_{21}(\theta,\theta')\right] \tag{5}$$

$$\kappa_{sh}(\theta) = \int_0^\pi d\theta' \sin\theta' \left[P_{12}(\theta,\theta') + P_{22}(\theta,\theta')\right] \tag{6}$$

where the phase matrix elements $P(\theta,\phi;\theta',\phi')$ are [5]:

$$\begin{aligned} P_{11}(\theta,\theta') = \int_0^{2\pi} & d(\phi-\phi')\cdot\delta\left[\cos^2\theta\cos^2\theta'\cos^2(\phi-\phi')\right.\\ & + 2\sin\theta\cos\theta\sin\theta'\cos\theta'\cos(\phi-\phi')\\ & \left. + \sin^2\theta\sin^2\theta'\right] W_{\nu\nu}(\theta,\theta';\phi-\phi') \end{aligned} \tag{7}$$

$$P_{22}(\theta,\theta') = \int_0^{2\pi} d\phi\cdot\delta\cos^2(\phi-\phi')W_{hh}(\theta,\theta';\phi-\phi') \tag{8}$$

$$P_{12}(\theta,\theta') = \int_0^{2\pi} d\phi\cdot\delta\cos^2\theta\sin^2(\phi-\phi')W_{\nu h}(\theta,\theta';\phi-\phi') \tag{9}$$

$$P_{21}(\theta,\theta') = \int_0^{2\pi} d\phi\cdot\delta\cos^2\theta'\sin^2(\phi-\phi')W_{h\nu}(\theta,\theta';\phi-\phi'), \tag{10}$$

where δ is the normalized variance of fluctuations (2). The function $W_{\alpha,\beta}$ can be obtained by [3]

$$W_{\alpha,\beta} = \frac{\pi k_{eff}^4 \delta}{2} \Phi(k_{eff}(\hat{k}_i - \hat{k}_s)), \tag{11}$$

where k_{eff} is the effective wave number in snow; $\hat{k}_i$ is the incident direction of incident plane wave; $\hat{k}_s$ is the scattered direction of scattered wave. The terms $\hat{k}_i - \hat{k}_s$ in (11) can be written in terms of $(\theta, \phi; \theta', \phi')$ as:

$$\begin{aligned}\hat{k}_i - \hat{k}_s &= \left[(\sin\theta\cos\phi - \sin\theta'\cos\phi')^2 + (\sin\theta\sin\phi - \sin\theta'\sin\phi')^2 \right. \\ &\quad \left. + (\cos\theta - \cos\theta')^2\right]^{1/2} \\ &= \sqrt{2}\left[1 - \cos\theta\cos\theta' - \sin\theta\sin\theta'\cos(\phi - \phi')\right]^{1/2}\end{aligned} \tag{12}$$

In (11), Φ is the spectral density function which is defined as the three-dimensional Fourier transform of the normalized correlation function $ACF(\overline{r}' - \overline{r}'')$

$$\Phi(\overline{k}) = \frac{1}{8\pi^3}\int_{-\infty}^{\infty} d^3\overline{r} ACF(\overline{r}) e^{i\overline{k}\cdot\overline{r}} \tag{13}$$

In the spherical symmetric case with exponential correlation function [10]:

$$ACF(|\overline{r}|) = \exp\left(-\frac{|\overline{r}|}{l_s}\right) \tag{14}$$

where l_s is correlation length. By substituting (14) to (13), we obtain:

$$\begin{aligned}\Phi(\overline{k}) &= \frac{1}{8\pi^3}\int_{-\infty}^{\infty} d^3\overline{r} \exp\left(\frac{|\overline{r}|}{l_s}\right) e^{i\overline{k}\cdot\overline{r}} \\ &= \frac{1}{8\pi^3}\int_0^{2\pi} d\phi \int_0^{\pi} \sin\theta d\theta \int_{-\infty}^{\infty} dr r^2 \exp\left(-\frac{r}{l_s}\right) e^{ikr} \\ &= \frac{1}{8\pi^3}\cdot 2\pi \cdot 2 \cdot \int_{-\infty}^{\infty} dr r^2 \exp\left(-\frac{r}{l_s}\right) e^{ikr}\end{aligned} \tag{15}$$

The integral in (15) is a one-dimensional Fourier transform of the function $f(r) = r^2\exp(-r/l_s)$ and the result is [11]:

$$\int_{-\infty}^{\infty} dr r^2 \exp\left(-\frac{r}{l_s}\right) e^{ikr} = 2l_s^3\Gamma(3)\frac{1}{(1 + k^2 l_s^2)^{3/2}}\cos\left[3\arctan(kl_s)\right] \tag{16}$$

where the Gamma function $\Gamma(3) = 2$. $W_{\alpha,\beta}$ can be written as:

$$W_{\alpha,\beta} = \frac{\pi k_{eff}^4 \delta}{2} \cdot \frac{1}{\pi^2} \cdot \frac{l_s^3}{\left(1 + \left[k_{eff}(\hat{k}_i - \hat{k}_s)\right]^2 l_s^2\right)^{3/2}} \cdot \cos\left[3 \arctan(k_{eff}(\hat{k}_i - \hat{k}_s) l_s)\right] \tag{17}$$

We can calculate the scattering coefficients as follows: According to the measurement procedure of [9] the incidence angle is $\theta = 0$. Applying the strong fluctuation theory with spherical symmetric correlation function, we can get from (7)–(10), (12) and (17):

$$W_{\alpha,\beta} = \frac{k_{eff}^4 \delta}{2} \cdot \frac{1}{\pi} \cdot \frac{l_s^3}{\left(1 + 2k_{eff}^2 \left[1 - \cos\theta'\right] l_s^2\right)^{3/2}} \cdot \cos\left[3 \arctan\left(k_{eff} 2^{1/2} \left[1 - \cos\theta'\right]^{1/2} l_s\right)\right] \tag{18}$$

$$P_{11}(\theta, \theta') = P_{12}(\theta, \theta') = \pi\delta \cos^2\theta' W_{\nu\nu} \tag{19}$$

$$P_{22}(\theta, \theta') = P_{21}(\theta, \theta') = \pi\delta W_{hh} \tag{20}$$

The scattering coefficients $\kappa_{s\nu}$ and κ_{sh} are deduced from the phase matrix components:

$$\kappa_{sv}(\theta) = \kappa_{sh}(\theta) = \int_0^{\pi} d\theta' 2\pi\delta \sin\theta' (1 + \cos^2\theta') W_{\nu\nu} \tag{21}$$

In numerical calculations discussed in Section 4, the correlation length is set to $l_s = 2D/3$ [10], where D is the mean diameter of ice particles.

For the non-spherical case, we consider anisotropic correlation function with azimuthal symmetry [5]:

$$ACF(r) = \exp\left(-\frac{x^2 + y^2}{L_p^2} - \frac{|z|}{L_z}\right) \tag{22}$$

The expression of the phase matrix elements $P(\theta, \phi; \theta', \phi')$ for anisotropic correlation function with azimuthal symmetry can be found in [5]. For easy reference, we give these phase matrix elements in Appendix I.

3. HALLIKAINEN ET AL.'S EXTINCTION COEFFICIENT MODEL

Hallikainen et al.'s [9] extinction coefficient model is:

$$\kappa_e = 2\mathrm{Im}(k_{eff}) = 2k_0\mathrm{Im}\left[\left(\frac{\varepsilon_{eff}}{\varepsilon_0}\right)^{\frac{1}{2}}\right] \tag{23}$$

where ε_{eff} is the effective permittivity of dry snow by using strong fluctuation theory with symmetric correlation function. The formulas for effective permittivity ε_{eff} with exponential correlation function are given in [7]. For easy reference, we give the formulas for effective permittivity in Appendix 2. In numerical calculations, the correlation length $l = 2D/3$ is used.

4. COMPARISON OF CALCULATED EXTINCTION COEFFICIENTS WITH DATA

The experimental data of snow extinction coefficient is adopted from [9]. According to [9], the snow extinction coefficient can be determined by measuring the transmission-loss factor $L(dB)$ as a function of the snow slab thickness. In [9], the transmission loss for 18 snow samples was measured at 18, 35, 60 and 90 GHz using a free-space transmission experiment system. During the measurements, the samples were handled and stored at $-15°$C. The properties of 18 snow samples and the experimental extinction coefficient κ_e for 18 snow samples can be found in [9]. For easy reference, the properties of 18 snow samples are listed in Table 1.

The comparison of calculated extinction coefficients with experimental data for 18 snow samples at 18 GHz, 35 GHz, 60 GHz and 90 GHz are shown in Fig. 1–4. In these Figures, "Hallikainen" means extinction coefficient calculated by using Hallikainen et al.'s extinction coefficient model (23); "Sphere" means extinction coefficient calculated by using strong fluctuation theory with spherical symmetric correlation function (21); "non-sphere" means extinction coefficient calculated by using strong fluctuation theory for anisotropic correlation function (22) with azimuthal symmetry [5].

It can be seen from Fig. 1–4 that the model predictions agree well with the measured extinction coefficients for 35 GHz and 60 GHz. The model derived values at 18 GHz are smaller than the measured

No.	Date	Depth snowpack	Observed Mean grain size (mm)	Surface roughness (mm)	Density g/cm^3	Dielectric constant at 10 GHz	comments
1	Feb. 1	Top	0.2	0	0.172	1.31	One-hour old snow
2	Feb. 15	Near Top	0.5	0	0.194	1.34	Newly fallen snow
3	Feb. 16	Near Top	0.7	0	0.217	1.39	Newly fallen snow
4	Feb. 18	Top	0.2	0	0.322	1.58	5-day old snow
5	Mar. 12	Top	0.3	0	0.277	1.52	
6	Mar. 12	Middle	0.9	0	0.268	1.49	Separate grains
7	Mar. 18	Near Top	0.4	0	0.235	1.41	Newly fallen snow
8	Mar. 21	Near Bottom	1.0	1	0.315	1.58	
9	Mar. 29	Top	1.0	1	0.385	1.75	Hard snow
10	Mar. 29	Near Bottom	1.0	1	0.276	1.50	Separate grains
11	Apr. 7	Top	1.3	2 to 3	0.307	1.61	
12	Apr. 11	Top	1.2	3	0.304	1.61	
13	Apr. 11	Near Bottom	1.3	1 to 3	0.293	1.54	
14	Apr. 13	Top	1.5	2 to 3	0.345	1.64	
15	Apr. 13	Middle	1.1	1 to 2	0.332	1.63	
16	Apr. 16	Bottom	1.1	1 to 2	0.361	1.77	Separate grains
17	Apr. 17	Top	1.5	2 to 4	0.390	1.79	
18	Apr. 30	Near Top	1.6	2 to 3	0.351	1.66	

Table 1. Properties of 18 snow samples [9].

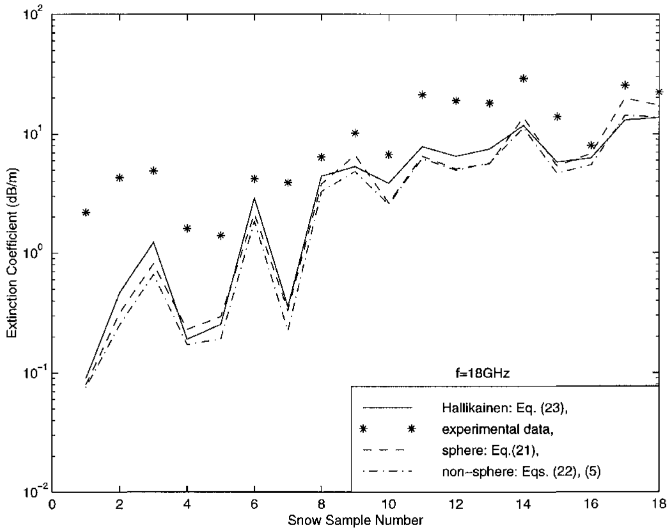

Figure 1. Extinction coefficient for 18 snow types of 18 GHz.

extinction coefficients. However, the experimental values of extinction coefficients at 18 GHz may be biased, due to the low transmission loss (mostly below 1 dB) even for thick snow samples [9]. At 90 GHz, the results of the models fit into the measured extinction coefficients for grain sizes smaller than 0.9 mm (samples 1–8). The model derived values are larger than the measured extinction coefficients for grain sizes larger than 0.9 mm (samples 9–18).

5. CONCLUSIONS

Extinction behaviors of dry snow by using the strong fluctuation theory are studied in this paper. We present two extinction coefficient models in this paper: one is derived from the phase matrix, the other is derived from the effective permittivity. Comparisons of calculated extinction coefficients with literature based data up to 90 GHz [9] are made. The results show that the strong fluctuation theory provides reasonably accurate results for the extinction coefficients except for large grain sizes at very high frequency (90 GHz). Moreover, we know indirectly that the effective permittivity calculated by strong fluctuation theory [6] is accurate enough in the microwave range. Therefore, the matrix and extinction coefficients derived in this paper and the effective permittivity derived by Stogryn [6] can be used in the radiative transfer equation to calculate the brightness temperature of a snowpack.

APPENDIX I: PHASE MATRIX ELEMENTS FOR THE TRANSVERSE ISOTROPIC CORRELATION FUNCTIONS

The elements of phase matrix for the transverse isotropic correlation functions can be written as [5]:

$$\begin{aligned} P_{11}(\theta,\theta') = Q(\theta-\theta')\exp(-A)\bigg\{ & \Big[\delta_{33}\sin^2\theta\sin^2\theta' \\ & +\frac{1}{2}\delta_{11}\cos^2\theta\cos^2\theta'\Big]I_0(A) \\ & +2\delta_{13}\sin\theta\sin\theta'\cos\theta\cos\theta' I_1(A) \\ & +\frac{1}{2}\delta_{11}\cos^2\theta\cos^2\theta' I_2(A)\bigg\} \end{aligned} \tag{A1}$$

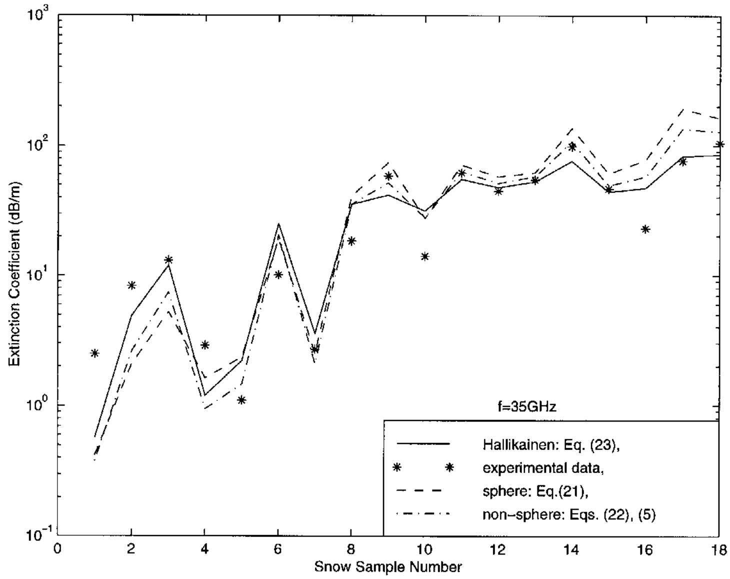

Figure 2. Extinction coefficient for 18 snow types of 35 GHz.

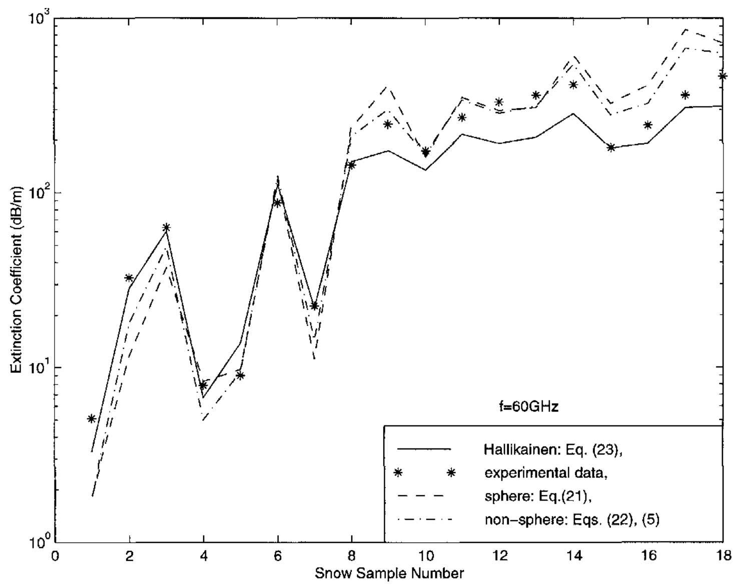

Figure 3. Extinction coefficient for 18 snow types of 60 GHz.

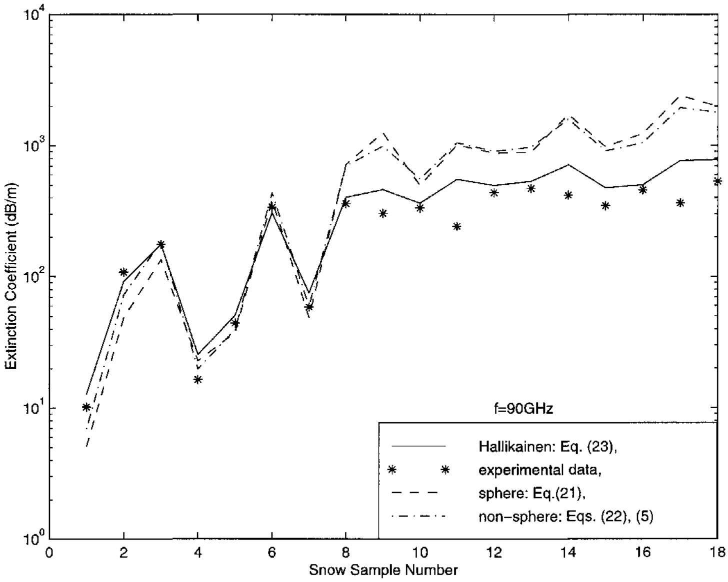

Figure 4. Extinction coefficient for 18 snow types of 90 GHz.

$$P_{12}(\theta,\theta') = \frac{1}{2}\delta_{11}Q(\theta,\theta')\exp(-A)\cos^2\theta\,[I_0(A) - I_2(A)] \tag{A2}$$

$$P_{12}(\theta,\theta') = \frac{1}{2}\delta_{11}Q(\theta,\theta')\exp(-A)\cos^2\theta'\,[I_0(A) - I_2(A)] \tag{A3}$$

$$P_{22}(\theta,\theta') = \frac{1}{2}\delta_{11}Q(\theta,\theta')\exp(-A)\,[I_0(A) + I_2(A)] \tag{A4}$$

where

$$Q(\theta,\theta') = \frac{k_g^4}{4}\frac{l_z l_p^2}{1 + k_g^2(\cos\theta - \cos\theta')^2 l_z^2}\exp\left[-\frac{k_g^2 l_p^2(\sin\theta - \sin\theta')^2}{4}\right] \tag{A5}$$

$$A = \frac{k_g^2 l_p^2 \sin\theta\sin\theta}{2} \tag{A6}$$

$$\delta_{11} = f_\nu \cdot \left|\frac{\varepsilon_s - \varepsilon_g}{\varepsilon_0 + S(\varepsilon_s - \varepsilon_g)}\right|^2 + (1 - f_\nu)\cdot\left|\frac{\varepsilon_b - \varepsilon_g}{\varepsilon_0 + S(\varepsilon_b - \varepsilon_g)}\right|^2 \tag{A7}$$

$$\delta_{13} = \mathrm{Re}\left[f_\nu \cdot \frac{\varepsilon_s - \varepsilon_g}{\varepsilon_0 + S(\varepsilon_s - \varepsilon_g)}\cdot\left\{\frac{\varepsilon_s - \varepsilon_{gz}}{\varepsilon_0 + S_z(\varepsilon_s - \varepsilon_{gz})}\right\}^*\right.$$

$$+(1-f_\nu)\cdot\frac{\varepsilon_b-\varepsilon_g}{\varepsilon_0+S(\varepsilon_b-\varepsilon_g)}\cdot\left\{\frac{\varepsilon_b-\varepsilon_{gz}}{\varepsilon_0+S_z(\varepsilon_b-\varepsilon_{gz})}\right\}^*\Bigg] \tag{A8}$$

$$\delta_{33}=f_\nu\cdot\left|\frac{\varepsilon_s-\varepsilon_{gz}}{\varepsilon_0+S_z(\varepsilon_s-\varepsilon_{gz})}\right|^2+(1-f_\nu)\cdot\left|\frac{\varepsilon_b-\varepsilon_{gz}}{\varepsilon_0+S_z(\varepsilon_b-\varepsilon_{gz})}\right|^2 \tag{A9}$$

and

$$S=\frac{\varepsilon_0\cdot b_1^{1/2}}{\varepsilon_g(2b_1^{1/2}+1)},\qquad S_z=\frac{\varepsilon_0}{\varepsilon_{gz}(2b_1^{1/2}+1)} \tag{A10}$$

where:

$$b_1=bh^2=\frac{\varepsilon_g\cdot l_z^2}{\varepsilon_{gz}\cdot l_p^2} \tag{A11}$$

ε_g and ε_{gz} are solutions of the two non-linear coupled equations [4]:

$$f_v\cdot\frac{\varepsilon_s-\varepsilon_g}{\varepsilon_0+S(\varepsilon_s-\varepsilon_g)}+(1-f_\nu)\cdot\frac{\varepsilon_b-\varepsilon_g}{\varepsilon_0+S(\varepsilon_b-\varepsilon_g)}=0 \tag{A12}$$

$$f_\nu\cdot\frac{\varepsilon_s-\varepsilon_{gz}}{\varepsilon_0+S_z(\varepsilon_s-\varepsilon_{gz})}+(1-f_v)\cdot\frac{\varepsilon_b-\varepsilon_{gz}}{\varepsilon_0+S_z(\varepsilon_b-\varepsilon_{gz})}=0 \tag{A13}$$

$I_n(A)$ is the modified Bessel Function of the first kind of n-th order, which can be calculated by:

$$I_n(z)=\frac{1}{\pi}\int_0^\pi \exp\left[z\cdot\cos\phi\right]\cos(n\phi)d\phi \tag{A14}$$

APPENDIX II: EFFECTIVE PERMITTIVITY ε_{eff} BY USING STRONG FLUCTUATION THEORY

Effective permittivity ε_{eff} by using strong fluctuation theory with exponential correlation function are [6]:

$$\varepsilon_{eff}=\varepsilon_g+k_0^2\delta\left(\frac{2I_1}{3}-\frac{iL_2}{k_g}-\frac{I_3}{3}+\frac{I_4}{k_0^2\varepsilon_g}\right) \tag{A15}$$

where

$$I_1=\frac{1}{\beta^2+k_g^2} \tag{A16}$$

$$I_2 = -\frac{3\beta}{2k_g^2} + \frac{1}{2k_g}\left(\frac{3\beta^2}{k_g^2} + 1\right)\tan^{-1}\frac{k_g}{\beta} \tag{A17}$$

$$I_3 = \frac{3}{k_g^2} - \frac{1}{\beta^2 + k_g^2} - \frac{3\beta}{k_g^3}\tan^{-1}\frac{k_g}{\beta} \tag{A18}$$

$$I_4 = \frac{1}{3} - \frac{\beta^2}{2k_g^2} - \frac{\beta}{2k_g}\left(\frac{\beta^2}{k_g^2} + 1\right)\tan^{-1}\frac{k_g}{\beta} \tag{A19}$$

with

$$\beta = \frac{1}{L} - ik_g \tag{A20}$$

where L is correlation length and the wave number $k_g = \omega\sqrt{\varepsilon_g \mu_0}$.

REFERENCES

1. Ulaby F., R. Moore, and A. Fung, *Microwave Remote Sensing, Vol. III,* Artech House, Inc., Norwood, 1986.
2. Fung, A. K., *Microwave Scattering and Emission Models and Their Applications,* Artech House, 1994.
3. Tsang, L., J. A. Kong, and R. T. Shin, *Theory of Remote Sensing,* Wiley Series in Remote Sensing, J. A. Kong (ed.), New York, 1985.
4. Tsang L., and J. A. Kong, "Scattering of electromagnetic waves for random media with strong permittivity fluctuations," *Radio Sci.,* Vol. 16, 303–320, 1981.
5. Jin, Y. Q., "The radiative transfer equation for strongly-fluctuation continuous random media," *J. Quant. Spectrosc. Radiat. Transfer,* Vol. 42, 529–537, 1989.
6. Stogryn, A., "A study of the microwave brightness temperature of snow from the point of view of strong fluctuation theory," *IEEE Trans. Geosci. Remote Sensing,* Vol. 24, No. 2, 220–231, 1986.
7. Stogryn, A., "The bilocal approximation for the effective dielectric constant of an isotropic random medium," *IEEE Trans. on Antennas and Propagation,* Vol. 32, No. 5, 517–520, 1984.
8. Nghiem, S. V., R. Kwok, J. A. Kong, R. T. Shin, S. A. Arcone, and A. J. Gow, "An electrothermodynamic model with distributed properties for effective permittivity of sea ice," *Radio Sci.,* Vol. 31, 297–311, 1996.
9. Hallikainen, M., F. Ulaby, and T. Deventer, "Extinction behavior of dry snow in the 18- to 90-GHz range," *IEEE Trans. Geosci. Remote Sensing,* Vol. 25, No. 6, 737–745, 1987.

10. Mätzler C., "Autocorrelation functions of granular media with free arrangement of spheres, spherical shells or ellipsoids," *J. Applied Physics,* Vol. 81, 1509–1517, 1997.
11. Oberhettinger, F., *Fourier Transforms of Distributions and Their Inverses, A Collection of Tables,* Academic Press, Inc., New York, 1973.